Published in final edited form as:
Neurobiol Aging. 2008 April ; 29(4): 524–541. doi:10.1016/j.neurobiolaging.2006.11.008.

Translational gene mapping of cognitive decline

Beth Wilmot[1,*], **Shannon K. McWeeney**[2], **Randal R. Nixon**[3], **Thomas J. Montine**[4], **Jamie Laut**[5], **Christina A. Harrington**[6], **Jeffrey A. Kaye**[5], and **Patricia L. Kramer**[1,5]

1*Department of Molecular and Medical Genetics, Oregon Health and Sciences University, Portland, OR, United States*

2*Division of Biostatistics, Department of Public Health and Preventive Medicine, Oregon Health and Sciences University, Portland, OR, United States*

3*Department of Pathology, Oregon Health and Sciences University, Portland, OR, United States*

4*Department of Pathology, University of Washington, Seattle, WA, United States*

5*Department of Neurology, Oregon Health and Sciences University, Portland, OR, United States*

6*Gene Microarray Shared Resource, Oregon Health and Sciences University, Portland, OR, United States*

Abstract

The ability to maintain cognitive function during aging is a complex process subject to genetic and environmental influences. Alzheimer's disease (AD) is the most common disorder causing cognitive decline among the elderly. Among those with AD, there is broad variation in the relationship between AD neuropathology and clinical manifestations of dementia. Differences in expression of genes involved in neural processing pathways may contribute to individual differences in maintenance of cognitive function.

We performed whole genome expression profiling of RNA obtained from frontal cortex of clinically non-demented and AD subjects to identify genes associated with brain aging and cognitive decline. Genetic mapping information and biological function annotation were incorporated to highlight genes of particular interest. The candidate genes identified in this study were compared with those from two other studies in different tissues to identify common underlying transcriptional profiles. In addition to confirming sweeping transcriptomal differences documented in previous studies of cognitive decline, we present new evidence for up-regulation of actin-related processes and down-regulation of translation, RNA processing and localization, and vesicle-mediated transport in individuals with cognitive decline.

Keywords

Cognitive reserve; cognitive decline; Alzheimer's disease; healthy brain aging; gene expression profiling; synaptic plasticity; Intersectin 1

*Corresponding Author: Beth Wilmot Dept. of Molecular and Medical Genetics L103 Oregon Health & Sciences University 3181 SW Sam Jackson Park Rd Portland, OR 97239 503-494-4362 503-494-7499 (fax) E-mail: wilmotb@ohsu.edu.
e-mail addresses of authors: Beth Wilmot: wilmotb@ohsu.edu Shannon K. McWeeney: mcweeney@ohsu.edu Randal R. Nixon: nixonr@ohsu.edu Thomas J. Montine: tmontine@u.washington.edu Jamie Laut: lautj@ohsu.edu Christina A. Harrington: harringc@ohsu.edu Jeffrey A. Kaye: kaye@ohsu.edu Patricia L. Kramer: kramer@ohsu.edu

1. Introduction

Finding the genes involved in a complex phenotype such as healthy brain aging is challenging due to the biological complexity of the underlying genetic and environmental components. A primary challenge is presented by the heterogeneity of the phenotype itself. Individuals exhibit broad variation in the ability to maintain cognitive function during the aging process. Clinically significant cognitive decline in the elderly is most commonly caused by Alzheimer's disease (AD). Diagnostic neuropathological features of AD include extracellular amyloid plaques and intracellular neurofibrillary tangles (NFTs). However, there is considerable neuropathological heterogeneity across individuals with clinical AD and individuals with no clinical signs of dementia, making division into "cases" and "controls" based on neuropathology problematic. In particular, there is tremendous variability in the relationship between the amount and location of AD neuropathology in the brain and the clinical manifestation of AD symptoms [61]. Individuals without loss of cognitive function may tolerate high levels of brain tissue injury presumptively indexed by amyloid plaques and NFTs, while others demonstrate loss of cognition with similar or even lower levels of lesion burden. These differences in protection from the effects of AD neuropathology may be due to genetic differences at several levels including the expression of gene products.

According to cognitive reserve theory, individuals differ in their capacity to maintain normative cognitive function and, accordingly, those with greater capacity are better equipped to delay or circumvent the damaging effects of brain lesions that in other less equipped individuals, lead to clinical manifestations of AD. The theory postulates that this natural variability across individuals is due to differences in neural processing mechanisms [32]. The physiological basis of this mechanism is unknown, although it is likely to reflect environmental as well as genetic factors [36,58]. Genetic variations can contribute to individual differences in normal cognitive function. Interaction between these genetic differences and environmental factors over the lifespan can amplify variation in cognitive function later in life.

There is growing evidence that variation in the quantity of a gene product, rather than simply presence or absence of product, can be responsible for the subtle effects of complex traits [21,30,62]. Several recent studies have shown that variation in gene expression is heritable [12,46,72] and can be mapped as a quantitative trait [46]. We suggest that differences in expression of genes in neural processing pathways are responsible for differences in the maintenance of cognitive function, and at least in part account for an important component of cognitive reserve.

To address this assertion, we performed whole genome expression profiling on a set of well-characterized, clinically non-demented and AD subjects in order to identify genes, or gene pathways, that contribute to cognitive decline. Subjects were stratified into four groups based on cognitive status prior to death (non-demented or AD) and neuropathological status defined by three categories of NFT burden (Braak stage I/II, III/IV, and V/VI) (Figure 1A). Non-demented subjects were represented in all three Braak-stage categories, whereas AD subjects were represented only in Braak stage V/VI. We designed three comparisons to test three hypotheses (Figure 1B). In the first comparison, we postulated that all non-demented subjects, taken as a whole (Groups 1, 2 and 3), would exhibit different gene expression profiles compared to AD subjects (Group 4), irrespective of NFT burden. We refer to this as the Extreme Cognitive Phenotypes Hypothesis (Hypothesis I). In the second comparison, we proposed that individuals with lower NFT burden (Braak stage I/II and III/IV, Groups 1 and 2) would display different expression profiles than those with higher NFT burden (Braak stage V/VI, Groups 3 and 4), irrespective of cognitive ability. We refer to this as the Neuropathologic Process Hypothesis (Hypothesis II). In the third comparison, we postulated that expression profiles in non-demented subjects with a high NFT burden (Group 3) would differ from those in AD subjects

with similar NFT pathology (Group 4). We refer to this as the Cognitive Reserve Hypothesis (Hypothesis III).

We interpret our gene expression results in the context of prior evidence from genetic linkage studies and biological function annotations to identify possible candidate susceptibility genes. Furthermore, since genes that are differentially expressed across tissues involved in AD pathology would provide valuable insight into common underlying genetic mechanisms in brain aging, we compared genes identified in this study, using frontal cortex, with genes identified in two other expression studies using hippocampus [8] and entorhinal cortex [20] . Genes that were differentially expressed across the three studies, emphasizing common themes of pathology underlying dementia, are key candidates for further studies of genetic risk factors for cognitive decline.

2. Materials and methods

2.1 Patient and control samples

Postmortem human brain tissue comprised primarily of gray matter from frontal cortex was obtained from the neuropathology core of the NIA-Layton Aging and Alzheimer's Disease Center, Oregon Health & Sciences University (OHSU). All subjects were characterized based on specific clinical and neuropathologic criteria [43] through studies performed by the NIA-Layton Aging and Alzheimer's Disease Center. An extensive collection of clinical data, including cognitive and functional measures, and neuropathologic data was available for all subjects. Testing included annual cognitive, functional and neuropsychological examinations. At autopsy, portions of the brain were frozen at −80°C and the remainder was prepared for histological examination by fixation in 10% formalin. All subjects were scored for neuritic amyloid plaques and neurofibrillary tangles according to NIA-Reagan criteria [1,43].

All subjects met the following minimal criteria for study inclusion: post-mortem interval < 24 hours, neurological examination within one year of death, Caucasian, non-detectable cancer metastases, and minimal degradation of brain-derived RNA for microarray analysis (see below). AD subjects were also required to have age at onset > 70 years and a clinical diagnosis of Probable AD. AD subjects with a coexisting neuropathologic diagnosis of Parkinson's disease, Lewy Body Dementia or Frontotemporal Dementia were excluded from the study. Non-AD subjects were required to have a clinical diagnosis of "non-demented", a CDR score of 0 and a Mini-Mental State Examination score (MMSE) > 25 (Table 1). Braak stage [9] was used to further define all subjects with respect to severity of neurofibrillary tangle burden (Figure 1A). The study sample comprised fourteen subjects (7 male, 7 female). Average age at death was similar across all groups (89.7 - 93.6 years). Non-demented subjects had an average MMSE score of 28.4; AD subjects had an average MMSE score of 14.4 (Table 1).

2.2 RNA isolation and hybridization

Approximately 500 mg of fresh frozen brain tissue from each individual was processed for total RNA using the RNeasy kit (Qiagen Inc., Valencia, CA). RNA quality was assessed by UV absorbance measurement and electrophoresis on RNA NanoChips using the 2100 Bioanalyzer (Agilent, Palo Alto, CA). Samples were considered acceptable for labeling and further processing if UV260/280 ratios were greater than 1.7 and Bioanalyzer profiles showed minimal degradation. For determination of degradation status, Bioanalyzer profiles were referenced to a simultaneously processed control of high quality RNA whose profile correlated with good performance on an Affymetrix GeneChip array (Gene Microarray Shared Resource, OHSU).

Two ug of total RNA from each subject was amplified and labeled using the AMC one cycle cDNA, Affy IVT amplification/labeling protocol following manufacturer's instructions (Affymetrix Inc., Santa Clara, CA). Labeled targets were hybridized with Affymetrix GeneChip HG-U133 Plus 2.0 arrays. These arrays contain 47,000 transcripts spanning the entire human transcriptome. Sample labeling and array hybridizations and processing were performed in the Affymetrix Microarray Core, Gene Microarray Shared Resource, OHSU.

2.3 Realtime RT-PCR

Confirmation of array results was performed using TaqMan chemistry in qRT-PCR. Phenotypic heterogeneity as well as RNA quality profoundly effect gene expression levels. Two additional non-demented subjects, conforming to the same rigorous phenotypic criteria, were included with the original set of subjects, in order to substitute for two non-demented subjects for which RNA had degraded in the interim between the microarray analysis and the validation procedure. Polyadenylated mRNA from the total RNA isolated from frontal cortex was reverse transcribed (Transcriptor RT, Roche Diagnostics Corp, IN) using oligo dT primers (Invitrogen, CA). Specific primers corresponding to the short form of ITSN1 (Hs00495035_g1, Applied Biosystems, TX) were combined with cDNA and dNTPs in a master mix (FastStart DNA Master Hybrid Probes, Roche Diagnostics Corp, IN) and amplified by PCR in a SmartCycler (Cepheid, CA). Human mRNA (Ambion, Inc, Tx), treated in the same manner was used as the control sample. Because standard housekeeping genes displayed variable expression levels across sample groups, qRT-PCR reference genes were chosen from the results of the HG-U133 Plus 2.0 arrays. Two different genes (POL2RF, RTN2) were chosen based on their lack of differential expression across groups and for their relative levels of expression similar to ITSN1 in the non-demented group. Samples were run in triplicate and the efficiency for each reaction was determined based on linear regression analysis of the exponential phase of the reaction [55]. Relative gene expression of ITSN1 to each reference gene was calculated using the efficiencies and crossing threshold (Ct) of each reaction [52]:

$$\text{Relative Ratio}=\text{Efficiency}_{\text{ITSN1}}^{(\text{Ct control}-\text{Ct sample})}/\text{Efficiency}_{\text{reference}}^{(\text{Ct control}-\text{Ct sample})}$$

2.4 Statistical analysis

An overview of the entire analytical work flow is provided in Figure 2. Statistical analyses were performed in the R v2.0.1 system for statistical computation ([68], http://www.R-project.org). Packages included in the Bioconductor v1.6 suite of analysis tools for genomic data [24] were utilized for specific analyses, as well as custom scripts.

Hybridized arrays were rigorously evaluated for quality using the *Affy* package v1.5.8 [23] of the Bioconductor project. Computer-generated graphs of the hybridization intensities across the chips allowed a visual assessment of the consistency of the hybridization reaction. Model-based normalization procedures were used to correct for systematic biases. Scatter plots [19] were used to compare the shapes of the distributions before and after normalization. Post-normalization residual plots were used to assess the model fit across all arrays.

Systematic errors cause technical variation which reduces the power of an array experiment to elucidate true biological variation. To minimize the impact of this variation on data analysis and biological interpretations [29], we used two different low level analysis approaches. Each data set was analyzed separately, allowing us to compare the impact of the low level routines on the downstream analysis. The Robust Multi-chip Analysis (RMA) [29] is a model-based pre-processing algorithm used to correct for probe-level differences. RMA in the *Affy* package was performed on log-transformed hybridization intensities using RMA background correction, quantile normalization and median polish as a summary statistic. The Variance

Stabilization and Calibration (VSN) [28] algorithm of the *Affy* package is a model-based normalization algorithm that specifically transforms the data such that the variance is independent of the mean intensity. The VSN algorithm was performed on intensity values and summarized using the median polish algorithm.

RMA and VSN processed data sets were analyzed to identify putative differentially expressed genes using Analysis of Variance (ANOVA) with the Linear Models for Microarray data analysis package (LIMMA v1.8.10) [63] of the Bioconductor project. Individual linear models were fitted for each transcript across the groups. The first two hypotheses were formally tested as planned comparisons within this framework.

Because each transcript is tested separately, and given the large number of transcripts on the array, the false positive error rate increases dramatically. Therefore, the q-value statistic [65], a minimum measure of the False Discovery Rate (FDR), was used to correct for multiple testing. The FDR is the number of predicted false positive results out of all significant tests. This measures the significance of each gene, taking into account that thousands of genes are being tested. Q-values were calculated from p-values generated in the LIMMA analysis using the QVALUE package v1.1 for R [65].

For each analysis, the final list of putative differentially expressed genes was defined as those probe sets with a q-value < 0.10 that occurred in both the RMA and VSN normalized data sets, in order to balance statistical rigor with maximal identification of candidate genes and given the discovery framework of this study.

It is noted that in the original experimental design, all three hypotheses were to be formally tested. However, during the QA/QC process for sample quality and hybridization, the loss of samples resulted in the third contrast being underpowered, leading to a different statistical approach for this comparison. Vector Projection is a dimension reduction technique for the rapid identification of genes with particular patterns of expression across groups (Terry Speed, Department of Statistics, University of California, Berkley, and Genetics and Bioinformatics, Walter and Eliza Hall Institute Australia; and Ingrid Lonnstedt, Department of Mathematics, Uppsala University, personal communication to S. McWeeney, [59]). It is useful as an initial exploratory data analysis tool, particularly when limited sample sizes preclude formal trend analysis, as was the case with Hypothesis III. Each gene has a vector of its normalized expression values across time. These values are projected onto the space spanned by the pattern of interest (vector of coefficients or weightings for group). In this case, the pattern of interest was a contrasting expression pattern between Cognitive Reserve (CR) and the other groups (i.e., identify genes up-regulated in CR and down-regulated in the other groups, or vice versa). Projection scores in the extreme tails of the normal Quantile-Quantile (QQ-plot) were used to identify transcripts with the best fit to the pattern of interest. The significance level was set at 0.1 for q-values in all expression analyses due to the gene discovery framework of this study

2.5 Determination of biological significance

All transcripts on the array were annotated for gene name, function, and chromosome location using NetAffx (http://www.affymetrix.com/analysis/index.affx, NCBI build 35). These annotations were then used for subsequent downstream analysis. For overrepresentation analyses (linkage, chromosome bands, GO), all significance levels were set at 0.05.

Transcripts that were differentially expressed in non-demented versus AD subjects (Hypothesis I) were analyzed for overrepresentation in specific chromosome regions in two ways. First, transcripts were annotated for cytogenetic bands and a χ^2 test of independence was performed to determine if there was evidence for association of transcript expression and cytogenetic band location. Secondly, transcripts were examined for their presence in a chromosomal region

known to be linked or associated with AD from previous studies. Concordant linkage/association regions were identified [6]. The number of differentially expressed transcripts located in these regions was compared to the number of transcripts in these regions on the Affymetrix HGU133 Plus 2 GeneChip array, using a one-tailed Fisher's exact test to determine if the number of differentially expressed transcripts located in each region was greater than that expected by chance.

Differentially expressed genes identified by ANOVA (q-value < 0.1) were assigned to Biological Process categories of the Gene Ontology (GO) Consortium (http://www.geneontology.org/ August, 2005). The GO is an international effort to define genes and their products using a controlled vocabulary. We used GOSTAT [3] to assess representation of differentially expressed genes in GO Biological Process categories. Identification of pertinent pathways depends on the availability of annotations mapped to the probe set. Differentially expressed genes were compared to all genes on the HG-U133Plus2 GeneChip array, using a 2 × 2 contingency table and counting the number of appearances of each category for differentially expressed genes versus reference genes. The probability that differentially expressed genes fall within a category more often than what would be expected by chance was calculated by χ^2 (Fisher's Exact test if the counts within a category are below 5). FDR was used to correct for multiple testing by controlling for interdependencies among the categories [4] given the hierarchical nature of the GO Ontology.

The Kyoto Encyclopedia of Genes and Genomes (KEGG) database (http://www.genome.jp/kegg/, September, 2005) was used to classify differentially regulated genes into canonical pathways for biological interpretation. Transcripts were annotated for their presence in a KEGG pathway and the significance of the number of genes differentially expressed in each pathway was determined by a one-tailed Fisher's Exact Test.

2.6 Identification of genes in common across tissues

Comparison of our study with two previously published gene profiling experiments [8,20] was used to identify genes that would reveal common pathophysiological mechanisms. First, differential gene expression related to cognitive decline was determined by combining transcripts differentially regulated in the comparisons of AD versus non-demented subjects in hippocampus [8], entorhinal cortex [20] and frontal cortex (this study). Because Blalock, et al [8] used the Affymetrix HG_U133A GeneChip array, we used a subset of data from the other two studies that corresponded to the Probe IDs found on the Affymetrix HG_U133A GeneChip. Significance was set at $p < 0.1$ for each data set and the intersection of Affymetrix Probe Ids was defined as the set of transcripts in common. It is noted that we cite p-values rather than q-values for this component as that is what was reported by the other studies. Because there are often multiple transcripts mapping to one gene on the GeneChip array, we also generated a data set of the intersection of differentially expressed genes in common among the three experiments using the annotated gene symbol. Secondly, we compared the transcripts involved in NFT formation (Hypothesis II) with the differentially expressed transcripts obtained by Dunckley et al. [20] from neurons without NFTs from AD subjects versus adjacent neurons with NFTs. The final data set of transcripts involved in NFT formation was defined to be the intersection of Affymetrix HG_U133Plus2 Probe IDs differentially expressed in both data sets.

3. Results

Putative differentially expressed transcripts were identified based on Hypothesis I (extreme cognitive phenotypes) and Hypothesis II (NFT formation) in order to identify genes involved in different, but overlapping, features of age-related pathological processes. Particular attention was focused on differentially expressed genes in chromosomal regions shown to be linked or associated with AD in previous studies [59]. In addition, we used the Gene Ontology (GO)

Biological Process categories to identify cellular events influenced by the differentially expressed genes associated with cognitive decline. For the probe sets identified in our analyses, only a subset had available GO annotations (Table 2). The overall level of available gene annotation was 32% of the unique genes annotated for GO Biological Process terms. Subsequent analyses are dependent on these annotations.

3.1 Extreme cognitive phenotypes

We identified 8346 transcripts, representing 5096 genes, that were differentially expressed ($q < 0.1$) between non-demented and AD subjects (Hypothesis 1, Figure 1B) (Supplemental Table 1). Cytogenetic band annotations were available for 6857 transcripts, of which 339 (4.9%) were located in regions with higher numbers of differentially expressed transcripts than expected by chance ($p < 0.05$, Supplemental Table 2). Ten cytogenetic bands contained more differentially regulated transcripts than would be expected by chance ($p < 0.05$, Supplemental Table 2).

All 8346 differentially expressed transcripts were annotated for location in a genomic region shown previously to be linked or associated with AD [6] (Supplemental Table 1). Of the total 8346, 873 transcripts were located within the sixteen linkage regions (Table 3). Of the transcripts up-regulated in AD, 264 are located in linkage regions. The most significant up-regulated transcript (35776_at) is the short form of Intersectin 1 (ITSN1), located in linkage region 21q22.1-q22.2. Affymetrix probe sets allow comparison of specific alternative transcripts in differential gene expression. For this gene, a different probe set interrogating the short form is also significantly up-regulated (209297_at, $q = 0.01$) but the long form is not differentially expressed ($q = 0.25$). These results were confirmed by qRT-PCR (Supplemental Figure 1) where the short form of ITSN1 is up-regulated in AD relative to two different reference genes ($p = 0.009$ and $p= 0.025$). The long form was not differentially expressed (data not shown). The most significant down-regulated transcript, ATP6V1G2, is also located in a linkage region, 6p21.3.

Cognitive decline, represented by AD subjects in our analysis, reveals a massive restructuring of cellular physiology (Table 4). Many of the most significant up-regulated categories are related to regulation of cellular functions. Categories related to transcription and its regulation, including chromatin modification, are among the most highly represented. Transcripts for actin-related processes and phosphate transport are also up-regulated.

Widespread down-regulation occurs in energy pathways and nucleic acid-related categories. Additionally, secretory pathways, RNA-related categories including splicing and mRNA processing, many pathways related to protein metabolism including folding, localization, targeting, transport and translation are down-regulated. Transcripts from genes involved in mitochondrial physiology are also down-regulated.

We utilized the KEGG database to place the differentially regulated genes into canonical pathways (Table 5). Of the 5096 differentially expressed genes, 226 were found to be clustered at levels greater than what would be expected by chance in 14 KEGG pathways. Of these, nearly half (45.5%) are involved in energy metabolism (oxidative phosphorylation, ATP synthesis, carbon fixation and CO_2 fixation). An additional 18% are involved in genetic information processing (transcription, translation and protein degradation). Carbohydrate (12.8%), amino acid (9.7%) and lipid (2.2%) metabolism are also represented. The percent of differentially expressed genes in each pathway (% abundance) varies from 37.2% - 71.4%. The pathway with the greatest percentage of differentially expressed genes (synthesis and degradation of ketone bodies) has the lowest number of total genes in the pathway. The pathway containing the greatest number of differentially expressed transcripts (50.7%) was oxidative phosphorylation.

3.2 Neurofibrillary tangle formation

We identified 528 transcripts, representing 492 genes, which were differentially expressed ($q < 0.1$) between subjects with low NFT pathology and those with high NFT levels (Hypothesis II, Figure 1B) (Supplemental Table 3). Of these, 98.9% were also differentially regulated in the Extreme Cognitive Phenotypes comparison. The six genes unique to Hypothesis II are close to the 0.1 threshold for significance (data not shown). A total of 49 transcripts were located in linked regions (Supplemental Table 3).

Overrepresentation in GO Biological Process categories reflected the dependence on current annotation. Specifically, the significant categories were dominated by a small number of well studied genes with pleiotropic effects (data not shown).

3.3 Cognitive reserve

Vector projection analysis allowed initial determination of putative candidate genes involved in cognitive reserve. Eleven transcripts, all located outside known AD linkage regions, were identified as possible candidates (Table 6). Of these, only one (GSTT1, involved in glutathione metabolism) was also differentially regulated in the Extreme Cognitive Phenotypes comparison. All other genes are unique to the Cognitive Reserve analysis.

3.4 Identification of common themes related to cognitive decline

We compared genes identified in this study, using frontal cortex, with genes identified in two other expression studies using hippocampus and entorhinal cortex. Blalock et al [8] compared hippocampal gene expression in non-demented and AD subjects stratified by severity of disease as measured by NFT count and MMSE scores. Dunckley et a l [20] used laser capture microdissection (LCM) to obtain RNA from neurons in entorhinal cortex, and then compared gene expression patterns in NFT-containing neurons and adjacent NFT-free neurons in AD subjects. Neurons without NFTs were also obtained from non-demented subjects for comparison.

In order to identify genes common to the underlying process of cognitive decline, we combined the data sets across the three different tissues (Table 7A and Table 8). Pairwise comparisons for all transcripts on the HG_U133A GeneChip array showed similar concordance with our data and either of the other data sets. Concordance rates among any two data sets varied between 7.1% and 20.8%. A total of 174 transcripts were concordant (FDR 10%) across all three data sets. More stringent criteria (FDR 5%) resulted in a loss of 30% of those transcripts. The overall concordance rate for differentially-regulated transcripts across all three data sets ranged from 1.0% - 3.9%. Of the 18 transcripts located in linkage regions (Table 8), six are involved in intracellular transport (ITSN1, ATP6V1G2, SYNJ1, SYNCRIP, DIRAS2) and three are related to mitochondria (ATP5J, ATP5C1, MRPS10). GO category analysis of the entire concordant transcript IDs demonstrated that the most significantly overrepresented GO category for up-regulated genes was signal transduction (data not shown). Down-regulated transcripts were most notably overrepresented in energy pathways and carbohydrate metabolism (data not shown). If the differentially expressed genes are mapped to gene symbol ID, the number of genes common to all three data sets increases (8.1-36.6%, FDR 10%) (Table 7B and Supplemental Table 4).

Dunckley et al [20] compared neurons with and without NFTs in AD subjects in order to investigate NFT formation. We compared low Braak stage subjects with high Braak stage subjects regardless of cognitive function for the same purpose. Transcripts differentially expressed in both data sets showed 39 (9.8%) concordant transcripts (Supplemental Table 5). Most are down-regulated in subjects with higher numbers of tangles (74.3%).

4. Discussion

Results of our human transcriptome profiling confirm many of the sweeping transcriptional differences associated with cognitive decline that have been previously documented, and implicate genes involved in transcriptional regulation, energy pathways, ion homeostasis dysregulation, apoptosis, and synaptic activity [8,14,20,37,73]. In addition, our results reveal significant up-regulation of actin-related processes and down-regulation of translation, RNA processing and localization, and vesicle mediated transport (Tables 4 and 5). This study identifies candidate genes, located in linkage regions, which had not been previously implicated in cognitive decline.

One difficulty with microarray results is that, because biochemical networks connect multiple physiological processes, a plausible biological mechanism for the implication of many genes can often be suggested. This is compounded when studying a complex trait impacting multiple cellular functions. We found that interpreting gene expression results in the context of genetic mapping studies and functional annotation allowed a more informed approach to identifying candidate genes in brain aging.

4.1 Extreme cognitive differences

We localized differentially expressed genes in healthy aging versus cognitive decline with reference to cytogenetic band annotations. In 14 genomic regions, more transcripts were differentially expressed than would be expected by chance (Supplemental Table 2), indicating possible co-regulation of genes in these regions by trans-acting factors. We identified functional changes of genes located in known AD linkage regions through differences in expression to identify cis-acting DNA polymorphisms. AD linkage regions did not overlap with the 14 genomic regions, indicating that the greater number of genes located within linkage regions was not coordinately regulated by trans-acting factors. The majority (87%) of transcripts were not found in linkage regions. However, differentially regulated genes located within the known AD linkage regions may contain cis-acting DNA polymorphisms that affect their gene expression and contribute to the linkage signal. Our results identified 873 possible candidate transcripts.

Biological annotation of these transcripts revealed that a number of these genes are involved in synaptic dysfunction, which has been shown to be an early process in cognitive decline. Synapse loss correlates positively with cognitive decline and indeed may occur prior to clinical signs [60]. Enlarged endosomes appear early in the course of AD pathology and are not present in healthy aging [11]. While many synapse-specific genes and vesicle-mediated transport genes are generally down-regulated in our study, we have identified a significantly up-regulated transcript, ITSN1, which is located in linkage region 21q22 (Supplemental Table 1). ITSN1 has not been studied in cognitive decline, although it has been postulated that ITSN1 might affect APP processing [48] and vesicular trafficking in AD [33]. Analysis of the other published data sets also identified ITSN1 as consistently up-regulated (Supplemental Table 4).

ITSN1 is a scaffold protein involved in synaptic vesicle recycling [42] and caveolae internalization [53]. Overexpression of ITSN1 blocks clathrin-mediated endocytosis [54], internalization of caveolae [53] and Ras activation [69] (Figure 3). Inhibition of endocytosis has been shown to increase soluble APP alpha release [10,13,57]. The fundamental significance of ITSN1 is its role in linking the endocytic machinery at the synapse with both the actin cytoskeleton and signal transduction pathways. Signaling pathways are regulated through ITSN1 binding of SOS and activation of RAS [69] and Elk1 activation through a RAS-independent process involving JNK[45]. Rho/Ras signaling is related to actin cytoskeleton through the protein kinase ROCK1 [38] that is also up-regulated in AD brain tissue (Supplemental Tables 1 and 4). The consistent findings across expression studies and the

functional consequences of its overexpression provide compelling evidence for a central role for ITSN1 in the pathogenic mechanisms of cognitive decline.

Down-regulated transcripts include many genes involved in synaptic function (Supplemental Table 1) including synaptojanin 1 (SYNJ1) located in linkage region 21q22.2. The most significantly down-regulated transcript across all brain tissues is ATP6V1G2 (Supplemental Tables 1 and 4) located in linkage region 6p21.3. ATP6V1G2 is a membrane bound vacuolar-type ATPase that maintains the acidity of lysosomal vesicles [67]. Luminal acidification by V-ATPases is required for proper intracellular vesicle sorting and degradation of endocytosed proteins. The relationship of ATP6V1G2 to the regulation of synaptic vesicle recycling or brain aging is unknown.

In addition to appropriate retrograde transport of endosomes, synaptic plasticity is also dependent on the anterograde transport and localization of specific mRNA transcripts to the synapse. Protein synthesis occurring at the synapse is considered to be a fundamental part of healthy synaptic function. Dysregulation of microtubule subunits and molecular motors is seen in cognitive decline (Supplemental Table 1) and down-regulation of all aspects of RNA function and transport is widespread in cognitive decline (Table 4). Two transcripts related to proper mRNA localization and translation at the synapse are located in linked regions. Synaptotagmin binding, cytoplasmic RNA interacting protein (SYNCRIP, 6q14-15) is a component of mRNA granules [2] binding mRNA and ensuring proper anterograde transport [31]. SYNCRIP interacts with various isoforms of the membrane-bound synaptotagmin [44]. Molecular motor trafficking on microtubules is postulated to be blocked by protein aggregates [56]. Failure of protein aggregates to be degraded through ubiquitin-mediated proteolysis has been shown to occur in AD [17,35] and local protein degradation through the ubiquitin-proteosome pathway has been shown to affect synaptic plasticity [25]. Many transcripts involved in this pathway are down-regulated in cognitive decline (Supplemental Table 1). A recent study suggests that cell death due to polyglutamine protein aggregates can be reduced by overexpression of RNA binding protein 3 (RBM3) [34]. RBM3 and its related gene CIRBP are down regulated in AD (Supplemental Table 1). These proteins are involved in response to stress [71]. RBM3 is located in a linkage region (Xp11.2) and has recently been shown to decrease microRNA (miRNA) levels with a parallel increase in protein synthesis [18]. MicroRNAs are small, highly conserved RNA molecules that regulate the expression of messenger RNA by binding to the 3′-untranslated regions (3′-UTR). Each miRNA is thought to regulate multiple genes and miRNA regulation is thought to influence many diverse cellular processes [41]. The contribution of miRNA regulation to cognitive decline is unknown, although miRNAs are postulated to be involved in processes related to synaptic plasticity [40].

4.2 NFT formation

NFT formation precedes cognitive decline and is correlated with severity of dementia in AD [7]. We identified a subset of genes that were differentially regulated in non-demented versus AD subjects (Hypothesis I) and subjects with low versus high tangle burden (Hypothesis II) (Supplemental Table 3). Overall, fewer transcripts were related to NFT formation and these had higher q-values than transcripts identified in the comparison of Extreme Cognitive Phenotypes (Supplemental Tables 1 and 3). This relationship is evident in other gene profiling experiments in which more transcripts were correlated with cognitive scores than NFTs [8] and more transcripts were differentially expressed in non-demented versus AD neurons than in AD non-NFT neurons versus AD NFT neurons [20]. Genes identified in this comparison may be more relevant to initial stages of brain pathology during NFT formation.

4.3 Cognitive reserve

Discovery of genes involved in individual brain capacity to tolerate, or circumvent, neuropathologic damage during aging would increase our ability to predict risk of dementia and determine risk-reducing factors. Non-demented individuals with heavy NFT burden may have more versatile neuronal processing mechanisms than individuals who develop dementia [64]. Although the limited sample size precluded statistical analyses, exploratory data analysis uncovered several genes with different patterns of expression in these subjects (Table 6).

Non-demented individuals with high Braak scores (Group 3) exhibited increased expression of a ribosomal structural gene (RPS4Y1) and the neuropeptide receptor bombesin-like receptor 3 (BRS3), compared with non-demented subjects with lower Braak scores (Groups 1 and 2) and AD subjects (Group 4). Bombesin-like neuropeptides are a family of G-protein-coupled receptors that have pleiotropic physiological effects, such as increasing hypertension and insulin secretion, stimulating gastric secretion, and modulating smooth muscle contraction [49]. Mice lacking BRS3 show mild obesity associated with hypertension, impairment of glucose tolerance and insulin resistance[50]. Dysregulated glucose metabolism has been shown to occur in AD pathology[16,47]. Our results suggest the possibility that individual protection of brain tissue from the pathological effects of NFTs results from regulation of protein synthesis and glucose metabolism.

Of the genes that show lower expression in Group 3 subjects, one has been previously studied in AD. Glutathione S-transferase theta 1 (GSTT1) is involved in detoxification of environmental toxins, but its role in susceptibility to AD is inconclusive [5,66]. Two genes are possibly involved in inflammatory processes. S100A8 is a subunit of Calprotectin, a calcium- and zinc-binding protein up-regulated in many inflammatory conditions[26]. Neuronal pentraxin II (NPTX2) is postulated to be involved in uptake of pro-inflammatory molecules [27]. Rat NPTX2 is regulated by synaptic activity and promotes neuronal migration [70]. Rap guanine nucleotide exchange factor 2 (RAPGEF2) is also involved in synaptic physiology through binding to a synaptic scaffold protein, and is hypothesized to link synaptic plasma membrane vesicles with RAS signal transduction [51]. These results further illustrate the central roles of anti-inflammatory processes and regulation of synaptic activity in maintaining healthy neuronal function. Additional experiments with larger sample sizes will be required to confirm the role of these genes in protection from brain tissue damage.

4.4 Genes common to the pathological process across all tissues

Determination of concordance across three transcriptomal studies allowed us to identify 174 transcripts common to cognitive decline across entorhinal cortex, hippocampus and frontal cortex. Synaptic plasticity—related genes are dysregulated in all three tissues. Likewise, down-regulation of energy pathways and ubiquitin-mediated protein degradation is widespread. Genes that function in these pathways are likely to be important in processes underlying the development of AD pathology. It is important to note that differentially expressed transcripts unique to each study may be the result of tissue specificity or non-biological differences in study design. Continued comparisons across studies and tissues will allow us to further elucidate the underlying genetic mechanisms of cognitive decline.

4.5 General considerations for transcriptomal studies

Central to the interpretation of biological significance of a particular differentially expressed transcript is the quality of the annotations obtained from publicly available databases. Often, complete annotation is not available for all of the transcripts interrogated. The annotation that does exist is dynamic and constantly updated. Finally, while it is transcripts that are interrogated on the array, it is common practice to map these transcripts to a gene index (such as Unigene ID). There can often be a loss of information in such a mapping, as it ignores differences at the

transcript level. A case in point highlighted in this study is ITSN1, which is commonly found in two isoforms, a short form and a long form. Additionally, over 19 alternatively spliced forms have been identified. Affymetrix GeneChip arrays target both the short and long forms of ITSN1. In all three data sets, it was the short form only (Probe ID 35776_at) that was differentially expressed. This finding was confirmed with qRT-PCR. In the analysis of the microarray data, transcripts for the same gene are often seen as technical replicates, rather than biological variants, such that any gene with discordant ProbeSets is discarded from further analysis. This results in failure to detect unique isoforms and transcripts that may play a key role in the biological process under study.

This highlights an important aspect of the dynamic and complex nature of the annotation process that may not always be appreciated. There has been a great deal of recent debate concerning the reliability of microarray gene expression on the same samples across different platforms [22,39]. A key point that is often missed is that in order to compare the arrays, individual transcripts are mapped to gene indices, due to the fact that different transcripts are interrogated on different platforms. There is an inherent loss of information in this mapping as alternate transcripts (each potentially with different expression patterns) are all mapped to the same gene identifier. Attempting to determine concordance based on gene annotation (such as gene symbol, name or Unigene ID) can be misleading and give overestimates of discordance, as described above.

Validation studies of microarrays using qRT-PCR also can suffer from overestimates of discordance between the arrays and the RT-PCR when primers are not designed to the same targets as the array. Strong correlations are seen between qRT-PCR and microarray results when the same transcript targets are tested [15]. This is clearly demonstrated by ITSN1 in this study, where only one transcript variant is differentially expressed, making primer design even more critical. These issues need to be considered in design of new studies and meta-analysis of existing data.

5. Summary

We have described a gene profiling approach to dissecting the complex phenotypes involved in brain aging. Comparison of our results with two previously published studies using a comparable microarray platform revealed common pathways underlying cognitive decline in three different brain tissues. Novel genes in pathways previously recognized as crucial to healthy brain aging have been identified. Dysregulated genes that are both involved in known AD critical pathways and located in linkage/association regions represent potential candidates for gene association studies.

Supplementary Material

Refer to Web version on PubMed Central for supplementary material.

ACKNOWLEDGEMENTS

The Layton Aging and Alzheimer’s Disease Center, NIH grants P30AG08017 and M01RR034 (JK), P3005411 (TM), Medical Research Foundation of Oregon Grant #0418 (PK), Department of Veteran’s Affairs Merit Review Award (JK). Microarray assays were performed in the Affymetrix Microarray Core of the OHSU Gene Microarray Shared Resource.

Disclosure of funding. Dr. Harrington has a significant financial interest in Affymetrix, Inc. This potential conflict of interest has been reviewed and a management plan approved by the OHSU Conflict of Interest in Research Committee has been implemented.

Literature

[1]. Consensus recommendations for the postmortem diagnosis of Alzheimer's disease. The National Institute on Aging, and Reagan Institute Working Group on Diagnostic Criteria for the Neuropathological Assessment of Alzheimer's Disease. Neurobiol Aging 1997;18(4 Supp):S1–2. [PubMed: 9330978]

[2]. Bannai H, Fukatsu K, Mizutani A, Natsume T, Iemura S, Ikegami T, Inoue T, Mikoshiba K. An RNA-interacting protein, SYNCRIP (heterogeneous nuclear ribonuclear protein Q1/NSAP1) is a component of mRNA granule transported with inositol 1,4,5-trisphosphate receptor type 1 mRNA in neuronal dendrites. J Biol Chem 2004;279(51):53427–34. [PubMed: 15475564]

[3]. Beissbarth T, Speed TP. GOstat: find statistically overrepresented Gene Ontologies within a group of genes. Bioinformatics 2004;20(9):1464–5. [PubMed: 14962934]

[4]. Benjamini Y, Yekutieli D. The Control of the False Discovery Rate in Multiple Testing under Dependency. The Annal of Statistics 2001;29(4):1165–88.

[5]. Bernardini S, Bellincampi L, Ballerini S, Federici G, Iori R, Trequattrini A, Ciappi F, Baldinetti F, Bossu P, Caltagirone C, Spalletta G. Glutathione S-transferase P1 *C allelic variant increases susceptibility for late-onset Alzheimer disease: association study and relationship with apolipoprotein E epsilon4 allele. Clin Chem 2005;51(6):944–51. [PubMed: 15805147]

[6]. Bertram L, Tanzi RE. Alzheimer's disease: one disorder, too many genes? Human Molecular Genetics 2004;13 Spec No 1:R135–41. [PubMed: 14764623]

[7]. Bierer LM, Hof PR, Purohit DP, Carlin L, Schmeidler J, Davis KL, Perl DP. Neocortical neurofibrillary tangles correlate with dementia severity in Alzheimer's disease. Arch Neurol 1995;52(1):81–8. [PubMed: 7826280]

[8]. Blalock EM, Geddes JW, Chen KC, Porter NM, Markesbery WR, Landfield PW. Incipient Alzheimer's disease: microarray correlation analyses reveal major transcriptional and tumor Suppressor responses. Proc Natl Acad Sci USA 2004;101(7):2173–8. [PubMed: 14769913]

[9]. Braak H, Braak E. Argyrophilic grain disease: frequency of occurrence in different age categories and neuropathological diagnostic criteria. J Neural Transm 1998;105(89):801–19. [PubMed: 9869320]

[10]. Carey RM, Balcz BA, Lopez-Coviella I, Slack BE. Inhibition of dynamin-dependent endocytosis increases shedding of the amyloid precursor protein ectodomain and reduces generation of amyloid beta protein. BMC Cell Biol 2005;6:30. [PubMed: 16095541]

[11]. Cataldo AM, Peterhoff CM, Troncoso JC, Gomez-Isla T, Hyman BT, Nixon RA. Endocytic pathway abnormalities precede amyloid beta deposition in sporadic Alzheimer's disease and Down syndrome: differential effects of APOE genotype and presenilin mutations. Am J Pathol 2000;157(1):277–86. [PubMed: 10880397]

[12]. Cheung VG, Jen KY, Weber T, Morley M, Devlin JL, Ewens KG, Spielman RS. Genetics of quantitative variation in human gene expression. Cold Spring Harb Symp Quant Biol 2003;68:403–7. [PubMed: 15338642]

[13]. Chyung JH, Selkoe DJ. Inhibition of receptor-mediated endocytosis demonstrates generation of amyloid beta-protein at the cell surface. J Biol Chem 2003;278(51):51035–43. [PubMed: 14525989]

[14]. Colangelo V, Schurr J, Ball MJ, Pelaez RP, Bazan NG, Lukiw WJ. Gene expression profiling of 12633 genes in Alzheimer hippocampal CA1: transcription and neurotrophic factor down-regulation and up-regulation of apoptotic and pro-inflammatory signaling. J Neurosci Res 2002;70(3):462–73. [PubMed: 12391607]

[15]. Dallas PB, Gottardo NG, Firth MJ, Beesley AH, Hoffmann K, Terry PA, Freitas JR, Boag JM, Cummings AJ, Kees UR. Gene expression levels assessed by oligonucleotide microarray analysis and quantitative real-time RT-PCR -- how well do they correlate? BMC Genomics 2005;6(1):59. [PubMed: 15854232]

[16]. de la Monte SM, Wands JR. Review of insulin and insulin-like growth factor expression, signaling, and malfunction in the central nervous system: relevance to Alzheimer's disease. J Alzheimers Dis 2005;7(1):45–61. [PubMed: 15750214]

[17]. Dimakopoulos AC. Protein aggregation in Alzheimer's disease and other neuropathological disorders. Curr Alzheimer Res 2005;2(1):19–28. [PubMed: 15977986]

[18]. Dresios J, Aschrafi A, Owens GC, Vanderklish PW, Edelman GM, Mauro VP. Cold stress-induced protein Rbm3 binds 60S ribosomal subunits, alters microRNA levels, and enhances global protein synthesis. Proc Natl Acad Sci U S A 2005;102(6):1865–70. [PubMed: 15684048]

[19]. Dudoit S, Yang Y, Callow M, Speed T. Statistical methods for identifying differentially expressed genes in replicated cDNA microarray experiments. Statistica Sinica 2002;12:111–39.

[20]. Dunckley T, Beach TG, Ramsey KE, Grover A, Mastroeni D, Walker DG, Lafleur BJ, Coon KD, Brown KM, Caselli R, Kukull W, Higdon R, McKeel D, Morris JC, Hulette C, Schmechel D, Reiman EM, Rogers J, Stephan DA. Gene expression correlates of neurofibrillary tangles in Alzheimer's disease. Neurobiol Aging. 2005

[21]. Farrall M. Quantitative genetic variation: a post-modern view. Hum Mol Genet 2004;13(Supp 1):R1–7. [PubMed: 14962979]

[22]. Fathallah-Shaykh HM. Microarrays: applications and pitfalls. Arch Neurol 2005;62(11):1669–72. [PubMed: 16286538]

[23]. Gautier L, Cope L, Bolstad BM, Irizarry RA. affy--analysis of Affymetrix GeneChip data at the probe level. Bioinformatics 2004;20(3):307–15. [PubMed: 14960456]

[24]. Gentleman RC, Carey VJ, Bates DM, Bolstad B, Dettling M, Dudoit S, Ellis B, Gautier L, Ge Y, Gentry J, Hornik K, Hothorn T, Huber W, Iacus S, Irizarry R, Leisch F, Li C, Maechler M, Rossini AJ, Sawitzki G, Smith C, Smyth G, Tierney L, Yang JY, Zhang J. Bioconductor: open software development for computational biology and bioinformatics. Genome Biol 2004;5(10):R80. [PubMed: 15461798]

[25]. Hegde AN. Ubiquitin-proteasome-mediated local protein degradation and synaptic plasticity. Prog Neurobiol 2004;73(5):311–57. [PubMed: 15312912]

[26]. Hermani A, De Servi B, Medunjanin S, Tessier PA, Mayer D. S100A8 and S100A9 activate MAP kinase and NF-kappaB signaling pathways and trigger translocation of RAGE in human prostate cancer cells. Exp Cell Res 2006;312(2):184–97. [PubMed: 16297907]

[27]. Hsu YC, Perin MS. Human neuronal pentraxin II (NPTX2): conservation, genomic structure, and chromosomal localization. Genomics 1995;28(2):220–7. [PubMed: 8530029]

[28]. Huber W, von Heydebreck A, Sultmann H, Poustka A, Vingron M. Variance stabilization applied to microarray data calibration and to the quantification of differential expression. Bioinformatics 2002;18(Supp 1):S96–104. [PubMed: 12169536]

[29]. Irizarry RA, Bolstad BM, Collin F, Cope LM, Hobbs B, Speed TP. Summaries of Affymetrix GeneChip probe level data. Nucleic Acids Res 2003;31(4):e15. [PubMed: 12582260]

[30]. Jais PH. How frequent is altered gene expression among susceptibility genes to human complex disorders? Genet Med 2005;7(2):83–96. [PubMed: 15714075]

[31]. Kanai Y, Dohmae N, Hirokawa N. Kinesin transports RNA: isolation and characterization of an RNA-transporting granule. Neuron 2004;43(4):513–25. [PubMed: 15312650]

[32]. Katzman R, Terry R, DeTeresa R, Brown T, Davies P, Fuld P, Renbing X, Peck A. Clinical, pathological, and neurochemical changes in dementia: a subgroup with preserved mental status and numerous neocortical plaques. Ann Neurol 1988;23(2):138–44. [PubMed: 2897823]

[33]. Keating DJ, Chen C, Pritchard MA. Alzheimer's disease and endocytic dysfunction: Clues from the Down syndrome-related proteins, DSCR1 and ITSN1. Ageing Res Rev. 2006

[34]. Kita H, Carmichael J, Swartz J, Muro S, Wyttenbach A, Matsubara K, Rubinsztein DC, Kato K. Modulation of polyglutamine-induced cell death by genes identified by expression profiling. Hum Mol Genet 2002;11(19):2279–87. [PubMed: 12217956]

[35]. Layfield R, Lowe J, Bedford L. The ubiquitin-proteasome system and neurodegenerative disorders. Essays Biochem 2005;41:157–71. [PubMed: 16250904]

[36]. Lee JH. Genetic evidence for cognitive reserve: variations in memory and related cognitive functions. J Clin Exp Neuropsychol 2003;25(5):594–613. [PubMed: 12815498]

[37]. Loring JF, Wen X, Lee JM, Seilhamer J, Somogyi R. A gene expression profile of Alzheimer's disease. DNA Cell Biol 2001;20(11):683–95. [PubMed: 11788046]

[38]. Maekawa M, Ishizaki T, Boku S, Watanabe N, Fujita A, Iwamatsu A, Obinata T, Ohashi K, Mizuno K, Narumiya S. Signaling from Rho to the actin cytoskeleton through protein kinases ROCK and LIM-kinase. Science 1999;285(5429):895–8. [PubMed: 10436159]

[39]. Marshall E. Getting the noise out of gene arrays. Science 2004;306(5696):630–1. [PubMed: 15499004]

[40]. Martin KC, Kosik KS. Synaptic tagging -- who's it? Nat Rev Neurosci 2002;3(10):813–20. [PubMed: 12360325]

[41]. Mattick JS, Makunin IV. Small regulatory RNAs in mammals. Hum Mol Genet 2005;14 Spec No 1:R121–32. [PubMed: 15809264]

[42]. McPherson PS, Kay BK, Hussain NK. Signaling on the endocytic pathway. Traffic 2001;2(6):375–84. [PubMed: 11389765]

[43]. Mirra SS, Heyman A, McKeel D, Sumi SM, Crain BJ, Brownlee LM, Vogel FS, Hughes JP, van Belle G, Berg L. The Consortium to Establish a Registry for Alzheimer's Disease (CERAD). Part II. Standardization of the neuropathologic assessment of Alzheimer's disease. Neurology 1991;41 (4):479–86. [PubMed: 2011243]

[44]. Mizutani A, Fukuda M, Ibata K, Shiraishi Y, Mikoshiba K. SYNCRIP, a cytoplasmic counterpart of heterogeneous nuclear ribonucleoprotein R, interacts with ubiquitous synaptotagmin isoforms. J Biol Chem 2000;275(13):9823–31. [PubMed: 10734137]

[45]. Mohney RP, Das M, Bivona TG, Hanes R, Adams AG, Philips MR, O'Bryan JP. Intersectin activates Ras but stimulates transcription through an independent pathway involving JNK. J Biol Chem 2003;278(47):47038–45. [PubMed: 12970366]

[46]. Morley M, Molony CM, Weber TM, Devlin JL, Ewens KG, Spielman RS, Cheung VG. Genetic analysis of genome-wide variation in human gene expression. Nature 2004;430(7001):743–7. [PubMed: 15269782]

[47]. Mosconi L. Brain glucose metabolism in the early and specific diagnosis of Alzheimer's disease. FDG-PET studies in MCI and AD. Eur J Nucl Med Mol Imaging 2005;32(4):486–510. [PubMed: 15747152]

[48]. O'Bryan JP, Mohney RP, Oldham CE. Mitogenesis and endocytosis: What's at the INTERSECTIoN? Oncogene 2001;20(44):6300–8. [PubMed: 11607832]

[49]. Ohki-Hamazaki H, Iwabuchi M, Maekawa F. Development and function of bombesin-like peptides and their receptors. Int J Dev Biol 2005;49(23):293–300. [PubMed: 15906244]

[50]. Ohki-Hamazaki H, Watase K, Yamamoto K, Ogura H, Yamano M, Yamada K, Maeno H, Imaki J, Kikuyama S, Wada E, Wada K. Mice lacking bombesin receptor subtype-3 develop metabolic defects and obesity. Nature 1997;390(6656):165–9. [PubMed: 9367152]

[51]. Ohtsuka T, Hata Y, Ide N, Yasuda T, Inoue E, Inoue T, Mizoguchi A, Takai Y. nRap GEP: a novel neural GDP/GTP exchange protein for rap1 small G protein that interacts with synaptic scaffolding molecule (S-SCAM). Biochem Biophys Res Commun 1999;265(1):38–44. [PubMed: 10548487]

[52]. Pfaffl MW. A new mathematical model for relative quantification in real-time RT-PCR. Nucleic Acids Res 2001;29(9):e45. [PubMed: 11328886]

[53]. Predescu SA, Predescu DN, Timblin BK, Stan RV, Malik AB. Intersectin regulates fission and internalization of caveolae in endothelial cells. Mol Biol Cell 2003;14(12):4997–5010. [PubMed: 12960435]

[54]. Pucharcos C, Estivill X, de la Luna S. Intersectin 2, a new multimodular protein involved in clathrin-mediated endocytosis. FEBS Lett 2000;478(12):43–51. [PubMed: 10922467]

[55]. Ramakers C, Ruijter JM, Deprez RH, Moorman AF. Assumption-free analysis of quantitative real-time polymerase chain reaction (PCR) data. Neurosci Lett 2003;339(1):62–6. [PubMed: 12618301]

[56]. Salehi A, Delcroix JD, Swaab DF. Alzheimer's disease and NGF signaling. J Neural Transm 2004;111(3):323–45. [PubMed: 14991458]

[57]. Savdie C, Ferguson SS, Vincent JP, Beaudet A, Stroh T. Cell-type-specific pathways of neurotensin endocytosis. Cell Tissue Res 2005:1–17.

[58]. Scarmeas N, Stern Y. Cognitive reserve: implications for diagnosis and prevention of Alzheimer's disease. Curr Neurol Neurosci Rep 2004;4(5):374–80. [PubMed: 15324603]

[59]. Scearce LM, Brestelli JE, McWeeney SK, Lee CS, Mazzarelli J, Pinney DF, Pizarro A, Stoeckert CJ Jr. Clifton SW, Permutt MA, Brown J, Melton DA, Kaestner KH. Functional genomics of the endocrine pancreas: the pancreas clone set and PancChip, new resources for diabetes research. Diabetes 2002;51(7):1997–2004. [PubMed: 12086925]

[60]. Scheff SW, Price DA, Schmitt FA, Mufson EJ. Hippocampal synaptic loss in early Alzheimer's disease and mild cognitive impairment. Neurobiol Aging. 2005

[61]. Schmitt FA, Davis DG, Wekstein DR, Smith CD, Ashford JW, Markesbery WR. "Preclinical" AD revisited: neuropathology of cognitively normal older adults. Neurology 2000;55(3):370–6. [PubMed: 10932270]

[62]. Singleton A, Myers A, Hardy J. The law of mass action applied to neurodegenerative disease: a hypothesis concerning the etiology and pathogenesis of complex diseases. Hum Mol Genet 2004;13 Spec No 1:R123–6. [PubMed: 14976159]

[63]. Smyth G. Linear models and empirical bayes methods for assessing differential expression in microarray experiments. Statistical Applications in Genetics and Molecular Biology 2004;3(1):1–23.

[64]. Stern Y. What is cognitive reserve? Theory and research application of the reserve concept. J Int Neuropsychol Soc 2002;8(3):448–60. [PubMed: 11939702]

[65]. Storey JD, Tibshirani R. Statistical significance for genomewide studies. Proc Natl Acad Sci U S A 2003;100(16):9440–5. [PubMed: 12883005]

[66]. Stroombergen MC, Waring RH. Determination of glutathione S-transferase mu and theta polymorphisms in neurological disease. Hum Exp Toxicol 1999;18(3):141–5. [PubMed: 10215103]

[67]. Sun-Wada GH, Wada Y, Futai M. Diverse and essential roles of mammalian vacuolar-type proton pump ATPase: toward the physiological understanding of inside acidic compartments. Biochim Biophys Acta 2004;1658(12):106–14. [PubMed: 15282181]

[68]. Team, RDC. R: A Language and Environment for Statistical Computing. R Foundation for Statistical Computing. 2005. <http://www.R-project.org>

[69]. Tong XK, Hussain NK, Adams AG, O'Bryan JP, McPherson PS. Intersectin can regulate the Ras/MAP kinase pathway independent of its role in endocytosis. J Biol Chem 2000;275(38):29894–9. [PubMed: 10896662]

[70]. Tsui CC, Copeland NG, Gilbert DJ, Jenkins NA, Barnes C, Worley PF. Narp, a novel member of the pentraxin family, promotes neurite outgrowth and is dynamically regulated by neuronal activity. J Neurosci 1996;16(8):2463–78. [PubMed: 8786423]

[71]. Wellmann S, Buhrer C, Moderegger E, Zelmer A, Kirschner R, Koehne P, Fujita J, Seeger K. Oxygen-regulated expression of the RNA-binding proteins RBM3 and CIRP by a HIF-1-independent mechanism. J Cell Sci 2004;117(Pt 9):1785–94. [PubMed: 15075239]

[72]. Yan H, Yuan W, Velculescu VE, Vogelstein B, Kinzler KW. Allelic variation in human gene expression. Science 2002;297(5584):1143. [PubMed: 12183620]

[73]. Yao PJ, Zhu M, Pyun EI, Brooks AI, Therianos S, Meyers VE, Coleman PD. Defects in expression of genes related to synaptic vesicle trafficking in frontal cortex of Alzheimer's disease. Neurobiol Dis 2003;12(2):97–109. [PubMed: 12667465]

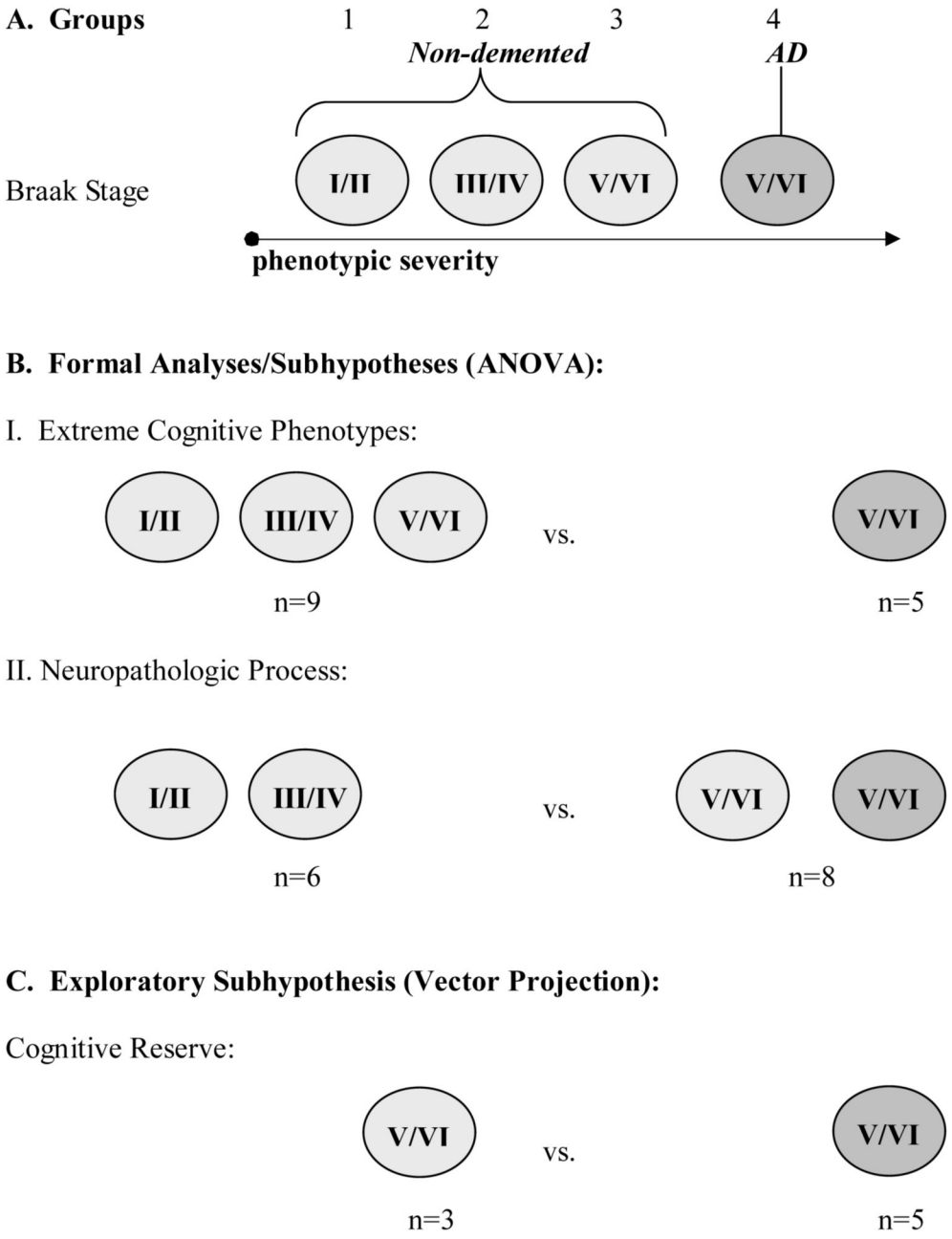

Figure 1. Subject Comparisons

A) Subjects were separated into four groups based on Braak stage and cognitive health. B) Two separate ANOVA comparisons performed. I. Extreme Cognitive Phenotypes were assessed by combining all non-demented subjects compared to AD subjects; II. Neuropathological Process was assessed by comparing low Braak stage subjects with high Braak stage subjects regardless of cognitive ability; III. Cognitive Reserve was assessed using Vector projection comparing non-demented, Braak V/VI subjects with AD subjects.

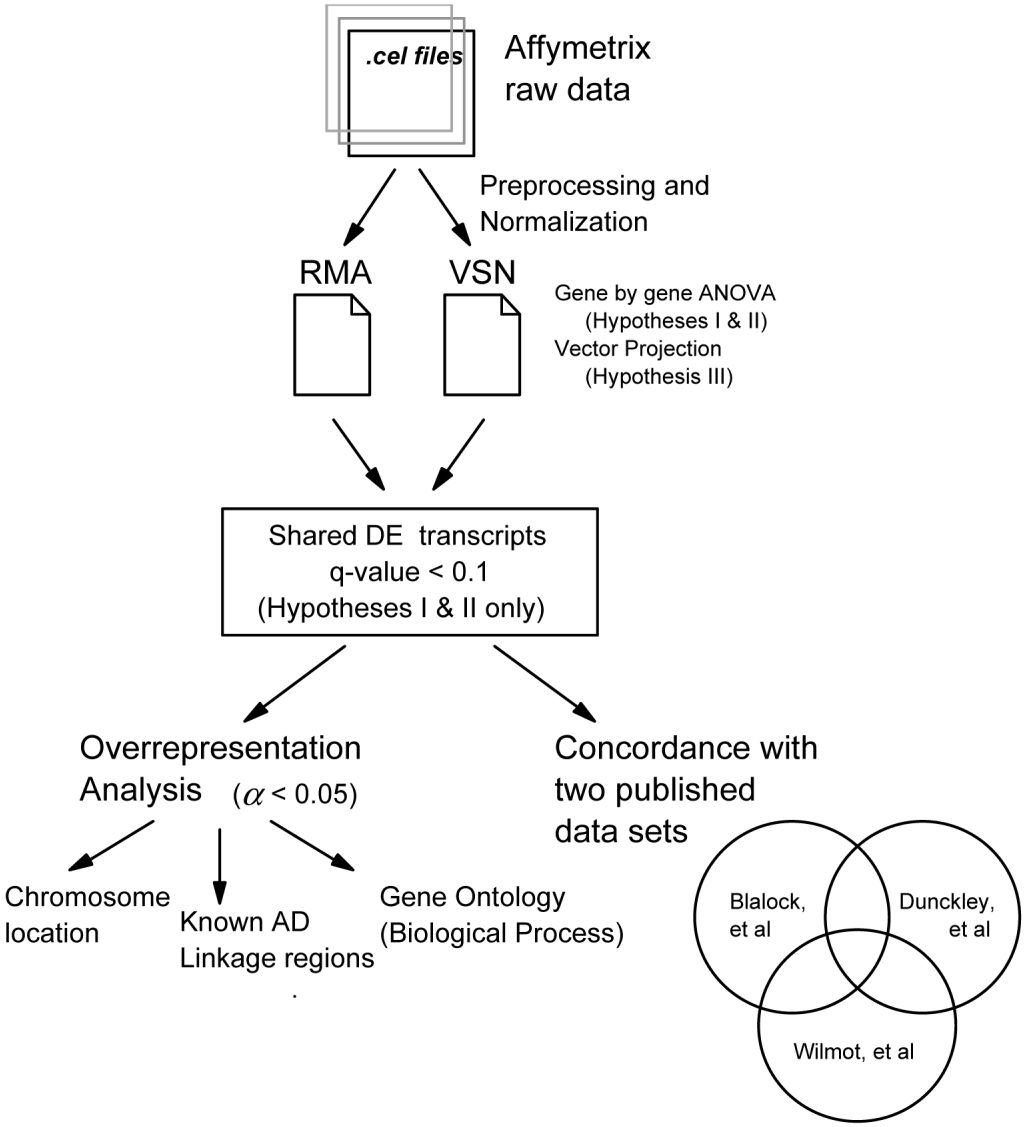

Figure 2. Analytical Work Flow

Raw data files were preprocessed and normalized using two different methods. Each data set was analyzed separately by ANOVA (Hypotheses I & II) and Vector Projection (Hypothesis III). Transcripts differentially expressed (DE) in both data sets (q-value < 0.1) were combined into one data set for downstream analysis. DE transcripts were analyzed by χ^2 for overrepresentation in categories of interest (chromosome location, known AD linkage regions and Gene Ontology Biological Process categories). Concordance of DE transcripts with two previous studies was investigated.

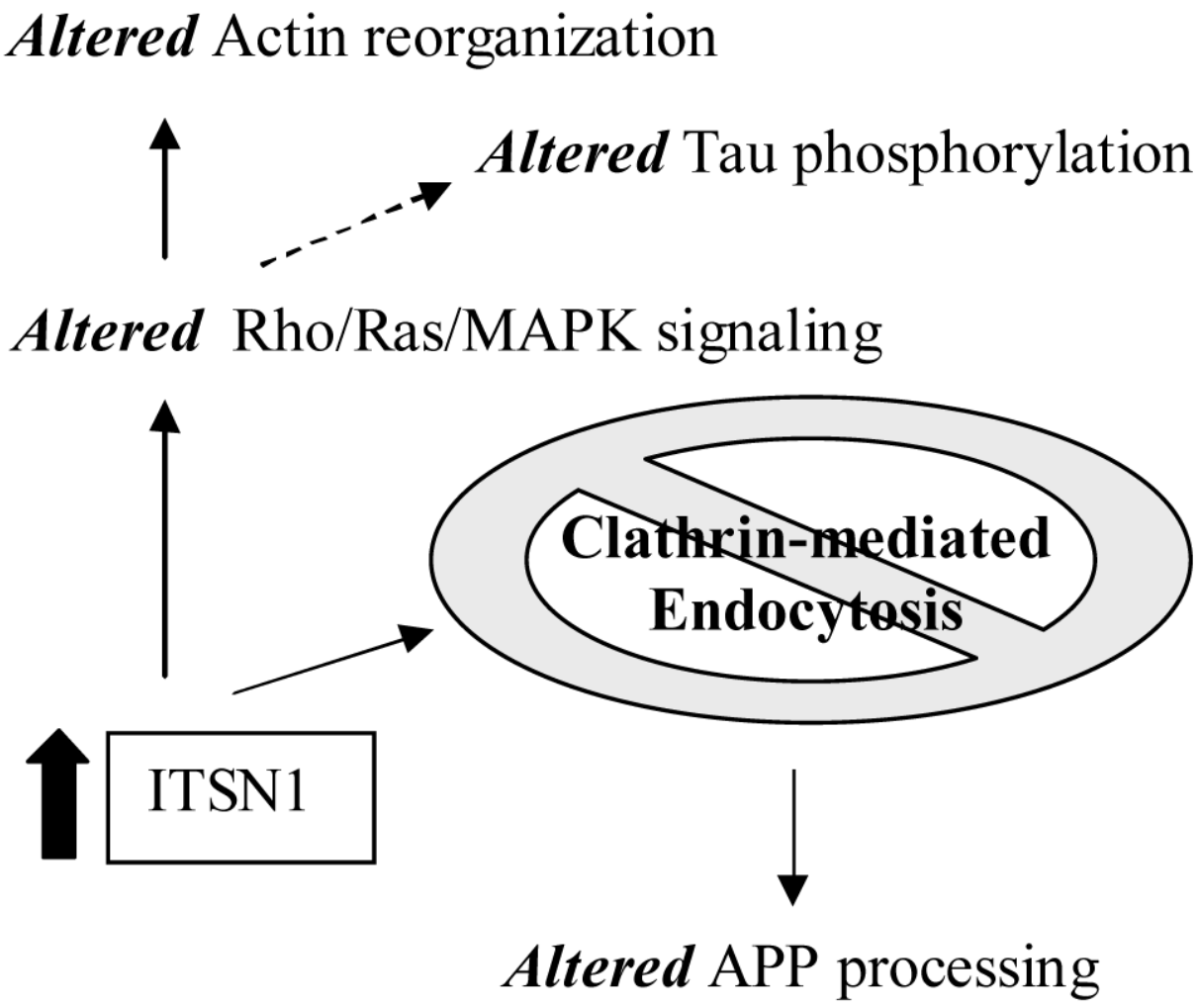

Figure. 3. Altered metabolism due to increased expression of Intersectin1
Solid arrows are direct consequences of higher levels of ITSN1 in published reports. Dashed arrow refers to the downstream effects of the MAPK signaling cascade on the phosphorylation of Tau.

Table 1

Subject Description

	Non-demented			AD
Braak	**I/II**	**III/IV**	**V/VI**	**V/VI**
Age	93.03 ± 12.19	90.85 ± 0.21	93.57 ± 1.59	89.74 ± 4.33
MMSE	28.0 ± 2.0	29.0 ± 1.41	28.33 ± 1.15	14.40 ± 6.99
Clinical DX	ND n=3	ND n=3	ND n=3	PRAD n=5

Subjects were assigned to four groups based on Braak stage scoring (see Methods). MMSE, Minimental Status Exam; Clinical DX, clinical diagnosis; ND, non-demented; Braak, Braak stage; n, number of subjects.

Table 2

Number of differentially expressed genes for each analysis[a]

	Up Regulated			Down regulated		
	Cognitive Differences	**NFT Formation**	**Cognitive Reserve**	**Cognitive Differences**	**NFT Formation**	**Cognitive Reserve**
Probe IDs[b]	3703	249	50	4643	279	31
Unique Genes	3664	249	48	4522	277	14
Annotated Genes	849 (23%)	41 (16%)	23 (47%)	1771 (39%)	117 (42%)	7 (50%)
GO IDs	4227	209	99	8211	520	44
Unique GO IDs	965	134	74	1544	271	41

[a] Gene Ontology (GO) Biological process category annotations for the differentially expressed genes in each analysis.

[b] Probe IDs, the number of Affymetrix Probe IDs that were differentially expressed in each analysis; Unique genes, the number of unique genes corresponding to the Probe IDs; Annotated Genes, the number of unique genes that have annotations associated with them in the GO database; GO IDs, the number of appearances of GO IDs associated with the annotated genes; Unique GO IDs, the number of unique GO IDs associated with the annotated genes. Numbers in paratheses indicate the percentage of unique genes that have associated GO annotations.

Table 3

Differentially expressed transcripts located in genomic regions linked to Alzheimer's disease[a]

Linkage Regions	# of transcripts		p-value[d]
	# DE[b]	# on chip[c]	
1p36	106	808	0.99
1q23-31	78	511	0.70
2p23-24	49	285	0.43
4q35	15	84	0.44
5p13-15	64	325	0.12
6p21	92	750	0.99
6q15-16	27	112	0.05
6q25-27	46	280	0.55
9p21	11	67	0.56
9q22	26	219	0.96
10q21-22	55	319	0.42
10q25	22	120	0.37
12p11-12	30	219	0.86
19q13	144	1256	1.00
21q21-22	66	499	0.96
Xp11-21	42	321	0.94

[a] Linkage regions are reproduced from Bertram and Tanzi [6]. Transcripts differentially expressed (DE) between non-demented and AD subjects (hypothesis I) were compared for overrepresentation in linkage regions.

[b] DE, number of transcripts differentially expressed at $q < 0.1$ by ANOVA that are located in the linkage region

[c] Number of transcripts on the chip that are located in the linkage region

[d] p-values are from Fisher's Exact test comparing transcripts DE at $q < 0.1$ to all transcripts on the Affymetrix HGU133Plus2 GeneChip in each linkage region.

Table 4

Biological process categories significantly overrepresented in Cognitive Differences Hypothesis (non-demented vs. AD)

A. up regulated in AD

Category	# genes DE[a]	# genes on chip[b]	FDR[c]
regulation of cellular physiological process	208	2252	3.21E-05
regulation of biological process	231	2578	3.21E-05
regulation of cellular process	215	2365	3.21E-05
regulation of physiological process	214	2376	6.34E-05
regulation of transcription, DNA dependent	149	1533	6.35E-05
regulation of transcription	154	1598	6.35E-05
regulation of nucleic acid metabolism	155	1620	8.39E-05
regulation of cellular metabolism	157	1650	8.94E-05
transcription	159	1684	0.000115
transcription, DNA-dependent	151	1587	0.000137
regulation of metabolism	159	1733	0.000752
negative regulation of cellular physiological process	48	384	0.0011
actin filament-based process	17	88	0.00146
negative regulation of physiological process	49	412	0.00451
negative regulation of cellular process	49	416	0.0059
chromatin modification	16	87	0.00717
actin cytoskeleton organization and biogenesis	16	77	0.0114
negative regulation of biological process	51	456	0.0189
phosphate transport	14	78	0.0363
nucleic acid metabolism	205	2502	0.0418

B. Down regulated in AD

Category	# genes	# genes on chip	FDR
coenzyme metabolism	65	124	1.69E-32
cofactor metabolism	70	145	1.42E-30
oxidative phosphorylation	41	65	2.47E-27
coenzyme biosynthesis	41	81	1.25E-18
cofactor biosynthesis	45	96	6.15E-18
biosynthesis	217	919	3.27E-17
ribonucleotide biosynthesis	34	69	1.76E-14
nucleoside phosphate metabolism	25	42	1.76E-14
ATP biosynthesis	25	42	1.76E-14
ATP coupled proton transport	23	38	1.30E-13
energy coupled proton transport, down electrochemical gradient	23	38	1.30E-13
ribonucleotide metabolism	34	72	1.58E-13

B. Down regulated in AD

Category	# genes	# genes on chip	FDR
ATP metabolism	25	44	1.76E-13
group transfer coenzyme metabolism	28	54	4.57E-13
ribonucleotide triphosphate biosynthesis	27	51	4.57E-13
purine ribonucleotide triphosphate biosynthesis	27	51	4.57E-13
purine nucleoside triphosphate biosynthesis	27	51	4.57E-13
nucleoside triphosphate metabolism	27	52	1.27E-12
generation of precursor metabolites and energy	128	504	1.33E-12
intracellular transport	114	433	1.63E-12
cellular biosynthesis	183	807	2.29E-12
ribonucleoside triphosphate metabolism	27	53	2.55E-12
purine ribonucleoside triphosphate metabolism	27	53	2.55E-12
purine nucleoside triphosphate metabolism	27	53	2.55E-12
purine ribonucleotide biosynthesis	30	64	7.52E-12
purine nucleotide biosynthesis	31	68	1.18E-11
nucleoside triphosphate metabolism	27	55	1.59E-11
establishment of protein localization	108	417	2.77E-11
purine ribonucleotide metabolism	30	66	3.22E-11
purine nucleotide metabolism	31	70	4.56E-11
purine nucleotide metabolism	107	415	4.80E-11
protein transport	42	113	1.10E-10
nucleotide biosynthesis	108	425	1.23E-10
hydrogen transport	29	65	1.86E-10
proton transport	28	64	1.19E-09
nucleotide metabolism	51	159	2.90E-09
intracellular protein transport	74	271	7.39E-09
aerobic respiration	18	27	5.76E-08
cellular respiration	18	29	3.12E-07
ATP synthesis coupled electron transport	16	25	1.28E-06
metabolism	933	6083	1.75E-06
translation	42	138	1.75E-06
RNA metabolism	82	340	1.75E-06
ATP synthesis coupled electron transport	15	23	2.41E-06
acety-CoA metabolism	15	24	5.36E-06
main pathways of carbohydrate metabolism	29	84	5.82E-06
energy derivation by oxidation of organic compounds	38	127	1.61E-05
tricarboxylic acid cycle	13	20	2.10E-05
acety-CoA catabolism	13	20	2.10E-05
coenzyme catabolism	13	20	2.10E-05
cofactor catabolism	14	23	2.23E-05
secretory pathway	35	116	3.75E-05
cellular metabolism	869	5712	6.16E-05

B. Down regulated in AD

Category	# genes	# genes on chip	FDR
macromolecule metabolism	462	2830	9.62E-05
RNA processing	63	266	0.000178
secretion	40	146	0.000178
protein folding	49	192	0.000189
mitochondrial electron transport, NADH to ubiquinone	12	20	0.000191
mRNA metabolism	44	167	0.000211
cellular macromolecule metabolism	436	2674	0.000251
cellular physiological process	1164	7955	0.000273
protein biosynthesis	95	455	0.000434
RNA splicing, via transesterif	26	83	0.000452
nuclear mRNA splicing, via spliceosome	26	83	0.000452
RNA splicing, via transesterif	26	83	0.000452
electron transport	70	312	0.000476
establishment of localization	305	1803	0.000597
mRNA processing	39	147	0.000626
transport	304	1801	0.000739
localization	305	1810	0.000823
RNA splicing	31	111	0.00151
protein targeting	31	111	0.00151
biopolymer metabolism	235	1361	0.00199
macromolecule biosynthesis	102	513	0.00205
Golgi vesicle transport	16	44	0.00229
protein-mitochondrial targeting	10	18	0.00292
sterol biosynthesis	12	25	0.00316
primary metabolism	815	5466	0.00606
protein metabolism	400	2514	0.00833
mitochondrial organization and biogenesis	8	14	0.0141
translational initiation	16	49	0.0175
cellular protein metabolism	394	2496	0.0193
inner mitochondrial membrane organization and biogenesis	5	6	0.0206
mitochondrial inner membrane protein import	5	6	0.0206
regulated secretory pathway	8	15	0.0248
quinone cofactor metabolism	4	4	0.0275
quinone cofactor biosynthesis	4	4	0.0275
ubiquinone biosynthesis	4	4	0.0275
ubiquinone metabolism	4	4	0.0275
lipid biosynthesis	39	170	0.036

[a] the number of differentially expressed genes (q< 0.1 by ANOVA) that are members of the category

[b] the number of genes on the Affymetrix GeneChip that are members of the category

[c] the FDR values are from χ^2 analysis corrected for multiple testing (see methods)

Table 5

Canonical Pathways involved in healthy aging

Pathway	# genes[a]	# genes in pathway[b]	p-value[c]	% A[d]
Oxidative phosphorylation	66	130	0.000	50.769
Proteasome	20	31	0.000	64.516
ATP synthesis	22	40	0.000	55.000
Infection	18	41	0.009	43.902
Citrate cycle (TCA cycle)	12	25	0.014	48.000
Synthesis and degradation of ketone bodies	5	7	0.015	71.429
RNA polymerase	11	23	0.019	47.826
Carbon fixation	10	22	0.037	45.455
Phenylalanine	6	11	0.041	54.545
Butanoate metabolism	17	44	0.044	38.636
Amyotrophic lateral sclerosis (ALS)	8	17	0.049	47.059
Reductive carboxylate cycle (CO2 fixation)	5	9	0.056	55.556
Valine	16	43	0.068	37.209
Aminoacyl-tRNA biosynthesis	10	25	0.088	40.000

[a] the number of differentially expressed genes ($q < 0.1$ by ANOVA) that are members of the pathway

[b] the total number of genes in the pathway

[c] p-values are from a one-tailed Fisher's Exact Test (see methods)

[d] % abundance of differentially expressed genes in that pathway

Table 6

Transcripts with maximum Differences between Group 3 (non-demented with high Braak score) and other Groups

Probe ID	Gene	Symbol	chromosome location
A. Transcripts with an increased transcript in non-demented, high Braak stage subjects.			
207369_at	bombesin-like receptor 3	BRS3	Xq26-q28
226558_at	hypothetical gene supported by AK096952; AK126241; BC068588	LOC441057	4p16.3
238774_at	Hypothetical protein LOC284058	LOC284058	17q21.31
201909_at	ribosomal protein S4, Y-linked 1	RPS4Y1	Yp11.3
B. Transcripts with a decreased transcript in non-demented, high Braak stage subjects.			
203815_at	glutathione S-transferase theta 1	GSTT1	22q11.23
224588_at			
227671_at			
203096_s_at	Rap guanine nucleotide exchange factor (GEF) 2	RAPGEF2	4q32.1
221728_x_at			
202917_s_at	S100 calcium binding protein A8 (calgranulin A)	S100A8	1q21
213479_at	neuronal pentraxin II	NPTX2	7q21.3-q22.1

Table 7

Concordance Rates per data set for Affymetrix HG_U133A GeneChip array.[a]

A. Intersection using Probe ID

	10% FDR		5% FDR	
	UP	DN	UP	DN
Blalock[b]	104 (8.4%)	493 (13.7%)	55 (9.4%)	392 (16.7%)
Dunckley	252 (20.4%)	733 (20.4%)	117 (19.9%)	488 (20.8%)
Blalock/Dunckley	451 (10.1%)	239 (8.4%)	254 (7.1%)	141 (10.0%)
all 3 data sets	33 (2.6%)	141 (3.9%)	6 (1.0%)	54 (2.3%)

B. Intersection using Gene Symbol

	10% FDR	
	UP	DN
Blalock[b]	258 (35.5%)	610 (27.5%)
Dunckley	195 (26.8%)	812 (36.6%)
Blalock/Dunckley	762 (21.7%)	554 (14.0%)
all 3 data sets	59 (8.1%)	274 (12.3%)

[a] Concordance was determined for each pair of data sets by measuring the intersection of transcripts significantly differentially regulated at 10% and 5% FDR. The number and percentage of transcripts concordant in each comparison is given.

[b] The concordance of each data set with our results, between Blalock, et al and Dunckley, et al, and the concordance among all three data sets is presented.

Table 8

Transcripts differentially expressed in non-demented versus demented that are common to all data sets.[a]

Upregulated in AD				
Probe ID	**Symbol**	**chromosome location**[b]	**p-value Blalock et al**	**p-value Dunckley et al**
35776_at	ITSN1	**21q22.1-q22.2**	0.05	0.00
201502_s_at	NFKBIA	14q13	0.01	0.00
202273_at	PDGFRB	5q31-q32	0.07	0.00
201125_s_at	ITGB5	3q21.2	0.00	0.02
202861_at	PER1	17p13.1-17p12	0.04	0.00
210473_s_at	GPR125	4p15.31	0.07	0.01
203685_at	BCL2	18q21.33, 18q21.3	0.00	0.07
	CHKB ///			
210069_at	CPT1B	22q13.33	0.02	0.06
206766_at	ITGA10	1q21	0.08	0.00
221527_s_at	PARD3	10p11.22-p11.21	0.02	0.04
212346_s_at	MXD4	4p16.3	0.08	0.02
213044_at	ROCK1	18q11.1	0.10	0.03
203505_at	ABCA1	9q31.1	0.01	0.01
36829_at	PER1	17p13.1-17p12	0.03	0.00
217937_s_at	HDAC7A	12q13.1	0.08	0.00
214594_x_at	ATP8B1	18q21-q22, 18q21.31	0.06	0.00
	DKFZP586A05			
209703_x_at	22	12q13.12	0.04	0.00
205168_at	DDR2	**1q12-q23**	0.00	0.04
	DKFZP434A01			
221191_at	31	7q11.23-q21.1	0.02	0.02
203080_s_at	BAZ2B	2q23-q24	0.07	0.04
	PRKX ///			
204060_s_at	PRKY	Xp22.3 , Yp11.2	0.00	0.01
	RHOQ ///			
212122_at	LOC284988	2p21 , 2q21.1	0.00	0.03
209370_s_at	SH3BP2	4p16.3	0.02	0.06
202724_s_at	FOXO1A	13q14.1	0.00	0.01
205111_s_at	PLCE1	10q23	0.03	0.00
205288_at	CDC14A	1p21	0.03	0.00
204061_at	PRKX	Xp22.3	0.02	0.00
202933_s_at	YES1	18p11.31-p11.21	0.02	0.03
209108_at	TM4SF6	Xq22	0.01	0.00

Downregulated in AD

Probe ID	Symbol	chromosome location	p-value Blalock et al	p-value Dunckley et al
214762_at	ATP6V1G2	**6p21.3**	0.01	0.02
221020_s_at	MFTC	8q22.3	0.06	0.00
210976_s_at	PFKM	12q13.3	0.02	0.04
219443_at	C20orf13	20p12.1	0.07	0.01
203889_at	SGNE1	15q13-q14	0.05	0.09
202325_s_at	ATP5J	**21q21.1**	0.09	0.03
201304_at	NDUFA5	7q32	0.01	0.09
204675_at	SRD5A1	5p15	0.08	0.00
222005_s_at	GNG3	11p11	0.03	0.00
200720_s_at	ACTR1A	10q24.32	0.06	0.00
208934_s_at	LGALS8	1q42-q43	0.02	0.01
218291_at	MAPBPIP	1q22	0.02	0.06
206290_s_at	RGS7	1q43	0.01	0.00
206489_s_at	DLGAP1	18p11.3	0.03	0.01
218488_at	EIF2B3	1p34.1	0.03	0.02
213849_s_at	PPP2R2B	5q31-5q32	0.01	0.02
215161_at	CAMK1G	1q32-q41	0.00	0.04
204471_at	GAP43	3q13.1-q13.2	0.03	0.00
200039_s_at	PSMB2	1p34.2	0.03	0.01
213011_s_at	TPI1	12p13	0.02	0.02
206055_s_at	SNRPA1	15q26.3	0.07	0.09
209583_s_at	CD200	3q12-q13	0.03	0.08
203218_at	MAPK9	5q35	0.09	0.09
211023_at	PDHB	3p21.1-p14.2	0.00	0.02
210027_s_at	APEX1	14q11.2-q12	0.02	0.03
221471_at	TDE1	20q13.1-13.3	0.02	0.01
218332_at	BEX1	Xq21-q23	0.06	0.00
213666_at	6-Sep	Xq24	0.00	0.03
210014_x_at	IDH3B	20p13	0.04	0.03
201569_s_at	CGI-51	22q13.31	0.07	0.00
211276_at	TCEAL2	Xq22.1-q22.3	0.02	0.00
202634_at	POLR2K	8q22.2	0.02	0.01
207142_at	KCNJ3	2q24.1	0.10	0.08
221482_s_at	ARPP-19	15q21.2	0.05	0.06
206342_x_at	IDS	Xq28	0.10	0.00
200822_x_at	TPI1	12p13	0.04	0.03
212990_at	SYNJ1	**21q22.2**	0.06	0.02
208870_x_at	ATP5C1	10p15.1	0.03	0.08
200613_at	AP2M1	3q28	0.03	0.00
218193_s_at	GOLT1B	**12p12.1**	0.08	0.00
217948_at	DKFZP564B147	Xq26.3	0.02	0.02

Downregulated in AD

Probe ID	Symbol	chromosome location	p-value Blalock et al	p-value Dunckley et al
202961_s_at	ATP5J2	7q22.1	0.10	0.02
202279_at	C14orf2	14q32.33	0.01	0.00
218404_at	SNX10	7p15.2	0.02	0.02
204744_s_at	IARS	9q21	0.05	0.04
202596_at	ENSA	1q21.2	0.00	0.09
209075_s_at	NIFUN	12q24.1	0.03	0.08
205549_at	PCP4	**21q22.2**	0.01	0.01
218813_s_at	SH3GLB2	9q34	0.07	0.01
208308_s_at	GPI	**19q13.1**	0.09	0.05
208745_at	ATP5L	11q23.3	0.04	0.04
200001_at	CAPNS1	**19q13.12**	0.10	0.07
208906_at	BSCL2	11q12-q13.5	0.08	0.08
206089_at	NELL1	11p15.2-p15.1	0.00	0.08
205711_x_at	ATP5C1	10p15.1	0.01	0.02
219196_at	SCG3	15q21	0.04	0.05
209025_s_at	SYNCRIP	**6q14-q15**	0.00	0.00
212826_s_at	SLC25A6	Xp22.32 and Yp	0.01	0.01
209482_at	POP7	7q22	0.04	0.08
211698_at	CRI1	15q21.1-q21.2	0.01	0.10
201849_at	BNIP3	10q26.3	0.03	0.00
201797_s_at	VARS2	**6p21.3**	0.04	0.07
205899_at	CCNA1	13q12.3-q13	0.08	0.07
201662_s_at	ACSL3	2q34-q35	0.04	0.02
209056_s_at	CDC5L	**6p21**	0.01	0.02
201524_x_at	UBE2N	12q22	0.01	0.04
219619_at	DIRAS2	**9q22.2**	0.04	0.06
206233_at	B4GALT6	18q11	0.05	0.00
213333_at	MDH2	7p12.3-q11.2	0.02	0.09
203079_s_at	CUL2	10p11.21	0.02	0.03
213902_at	ASAH1	8p22-p21.3	0.04	0.01
201400_at	PSMB3	17q12	0.02	0.01
215691_x_at	C1orf41	1p32.1-p33	0.01	0.00
217773_s_at	NDUFA4	7p21.3	0.01	0.05
201568_at	QP-C	5q31.1	0.06	0.02
206857_s_at	FKBP1B	**2p23.3**	0.08	0.00
214436_at	FBXL2	3p23	0.03	0.01
208977_x_at	TUBB2	6p25	0.03	0.06
200650_s_at	LDHA	11p15.4	0.01	0.00
216120_s_at	ATP2B2	3p25.3	0.01	0.00
212296_at	PSMD14	2q24.2	0.07	0.00
221437_s_at	MRPS15	1p35-p34.1	0.09	0.01

Downregulated in AD

Probe ID	Symbol	chromosome location	p-value Blalock et al	p-value Dunckley et al
201381_x_at	CACYBP	**1q24-q25**	0.07	0.00
206381_at	SCN2A2	2q23-q24	0.09	0.04
209849_s_at	RAD51C	17q22-q23	0.00	0.03
206949_s_at	RUSC1	1q21-q22	0.03	0.00
208975_s_at	KPNB1	17q21.32	0.04	0.08
210406_s_at	RAB6A ///	11q13.3 , 2q31	0.01	0.01
	RAB6C			
200027_at	NARS	18q21.2-q21.3	0.03	0.00
209914_s_at	NRXN1	2p16.3	0.08	0.02
214005_at	GGCX	2p12	0.06	0.00
201597_at	COX7A2	6q12	0.05	0.00
213366_x_at	ATP5C1	10p15.1	0.01	0.02
219073_s_at	OSBPL10	3p22.3	0.00	0.00
208905_at	CYCS	7p15.3	0.03	0.00
217801_at	ATP5E	20q13.32	0.03	0.05
202309_at	MTHFD1	14q24	0.00	0.00
203894_at	TUBG2	17q21	0.00	0.02
209877_at	SNCG	10q23.2-q23.3	0.02	0.09
216903_s_at	CBARA1	**10q22.1**	0.09	0.01
202260_s_at	STXBP1	9q34.1	0.08	0.00
201837_s_at	STAF65(gamma)	2pter-p25.1	0.00	0.00
218226_s_at	NDUFB4	3q13.33	0.06	0.00
207081_s_at	PIK4CA	22q11.21	0.02	0.07
209142_s_at	UBE2G1	1q42, 17p13.2	0.07	0.00
220045_at	NEUROD6	7p14.3	0.01	0.02
202090_s_at	UQCR	19p13.3	0.03	0.00
200734_s_at	ARF3	12q13	0.01	0.00
213726_x_at	TUBB2	6p25	0.02	0.04
201047_x_at	RAB6A	11q13.3	0.06	0.07
204141_at	TUBB2	6p25	0.02	0.00
210016_at	MYT1L	2p25.3	0.01	0.03
208936_x_at	LGALS8	1q42-q43	0.01	0.00
205691_at	SYNGR3	16p13	0.01	0.00
203001_s_at	STMN2	8q21.13	0.09	0.00
218732_at	Bit1	17q23.2	0.10	0.05
205113_at	NEF3	8p21	0.01	0.05
218106_s_at	MRPS10	**6p21.1-p12.1**	0.06	0.05
203846_at	TRIM32	9q33.1	0.01	0.00
209001_s_at	ANAPC13	3q22.1	0.02	0.00
203797_at	VSNL1	**2p24.3**	0.01	0.07
203303_at	TCTE1L	**Xp21**	0.05	0.00

Downregulated in AD				
Probe ID	**Symbol**	**chromosome location**	**p-value Blalock et al**	**p-value Dunckley et al**
211071_s_at	AF1Q	1q21	0.09	0.00
204247_s_at	CDK5	7q36	0.01	0.04
221288_at	GPR22	7q22-q31.1	0.01	0.07
201434_at	TTC1	5q32-q33.2	0.03	0.00
212976_at	TA-LRRP	1p22.2	0.03	0.07
203667_at	TBCA	5q14.1	0.01	0.05
200625_s_at	CAP1	1p34.2	0.02	0.00
218467_at	TNFSF5IP1	18p11.21	0.02	0.01
204465_s_at	INA	10q24.33	0.01	0.00
202754_at	R3HDM	2q21.3	0.02	0.01
215518_at	STXBP5L	3q13.33	0.05	0.00
222125_s_at	PH-4	3p21.31	0.02	0.02
206051_at	ELAVL4	1p34	0.09	0.03
202336_s_at	PAM	5q14-q21	0.10	0.00
202022_at	ALDOC	17cen-q12	0.02	0.08
201980_s_at	RSU1	10p13	0.01	0.01
211069_s_at	SUMO1	2q33	0.05	0.08
201527_at	ATP6V1F	7q32	0.06	0.05

[a] Differentially expressed transcripts are $q < 0.1$ from ANOVA

[b] Values in bold are chromosomal regions linked to AD